applied sciences

MDPI

Article

Statistical Modeling for PM_{10}, $PM_{2.5}$ and PM_1 at Gangneung Affected by Local Meteorological Variables and PM_{10} and $PM_{2.5}$ at Beijing for Non- and Dust Periods

Soo-Min Choi [1] and Hyo Choi [2,*]

[1] Department of Computer Engineering, Konkuk University, Chungju 27478, Korea; fuledoc@daum.net
[2] Atmospheric and Oceanic Disaster Research Institute, Gangneung 25563, Korea
* Correspondence: du8392@hanmail.net

Abstract: Multiple statistical prediction modeling of PM_{10}, $PM_{2.5}$ and PM_1 at Gangneung city, Korea, was performed in association with local meteorological parameters (air temperature, wind speed and relative humidity) and PM_{10} and $PM_{2.5}$ concentrations of an upwind site in Beijing, China, in the transport route of Chinese yellow dusts which originated from the Gobi Desert and passed through Beijing to the city from 18 March to 27 March 2015. Before and after the dust periods, the PM_{10}, $PM_{2.5}$ and PM_1 concentrations showed as being very high at 09:00 LST (the morning rush hour) by the increasing emitted pollutants from vehicles and flying dust from the road and their maxima occurred at 20:00 to 22:00 LST (the evening departure time) from the additional pollutants from resident heating boilers. During the dust period, these peak trends were not found due to the persistent accumulation of dust in the city from the Gobi Desert through Beijing, China, as shown in real-time COMS-AI satellite images. Multiple correlation coefficients among PM_{10}, $PM_{2.5}$ and PM_1 at Gangneung were in the range of 0.916 to 0.998. Multiple statistical models were devised to predict each PM concentration, and the significant levels through multi-regression analyses were $p < 0.001$, showing all the coefficients to be significant. The observed and calculated PM concentrations were compared, and new linear regression models were sequentially suggested to reproduce the original observed PM values with improved correlation coefficients, to some extent.

Keywords: PM_{10}; $PM_{2.5}$; PM_1; yellow dust; COMS-AI satellite images; correlation coefficient; multiple regression model

Citation: Choi, S.-M.; Choi, H. Statistical Modeling for PM_{10}, $PM_{2.5}$ and PM_1 at Gangneung Affected by Local Meteorological Variables and PM_{10} and $PM_{2.5}$ at Beijing for Non- and Dust Periods. *Appl. Sci.* **2021**, *11*, 11958. https://doi.org/10.3390/app112411958

Academic Editor: Harry D. Kambezidis

Received: 20 November 2021
Accepted: 12 December 2021
Published: 15 December 2021

1. Introduction

Atmospheric pollution consists of great amounts of different compounds, such as particulate matter and gas, mainly from vehicles and flying dusts on the road, industries, the burning of trash, forest fires and yellow dusts of the desert and arid areas to the atmosphere [1,2]. Generally, air pollutants are extremely harmful to the human body by reaching the lungs through the bronchi, which can cause respiratory, cardiovascular, and cerebrovascular disease [3–5].

The previous research studies mentioned that the particulate matter concentration in the ambient air of an urban area is greatly affected by not only meteorological parameters (air temperature, wind speed and direction, solar radiation, relative humidity and atmospheric pressure) [6–9], but also gaseous ones (CO, CO_2, O_3, SO_2, and NO_2) and so on [10–13]. Air pollution reduces visibility in smog and haze weather and influences the health threat to outdoor physical activity [14,15]. From numerical and experimental studies, it is well-known that, as meteorological conditions can promote or prevent the dispersion of air pollutants, the pollution state becomes much worse in atmospheric visibility [16].

During spring, when the wind speed is over 10 m/s and the relative humidity is less than 40% in the air near the surface of the Gobi Desert in southern Mongolia, the Kubuchi Desert in Inner Mongolia, the Ordos Desert, the Huangtu Plateau (the Loess Plateau) and

the Taklamakan Desert in northwest China, huge amounts of yellow sands and dusts are raised from the ground surface up to a 3 km or 5 km height, and they are vertically and horizontally transported to the wide downwind regions, such as eastern China, Korea, Japan and southeastern Asian countries. This phenomenon is referred to in a variety of ways: Huang Chen, KOSA, Asian Dust, Yellow Sand, Sand Storm and Dust Storm [17–22].

Due to the persistent accumulation of dust particles in the lower atmosphere of the source area, visibility during the dust period in China and Mongolia is the worst, and it becomes rapidly worse in the further downwind countries of northeast and southeast Asia, including China, Taiwan, Korea, Japan and even the west coast of the U.S.A. by the deposition of a huge amount of transported dusts [23–26]. Many environmental researchers have explained the chemical composition of fine and coarse particles in relation with Asian Dust events in detail [27–29].

Furthermore, Zhao [30] mentioned more severe air pollution in the case of a higher ratio of $PM_{2.5}/PM_{10}$ in China. Choi [31,32] and Lee and Chung [33] indicated that, using a simple regression method, the coarse particle concentration (PM_{10}–$PM_{2.5}$) in Gangneung city, Korea, was greater than the fine particle concentration ($PM_{2.5}$) during the dust period, and the coarse particulates larger than 2.5 μm could significantly contribute to the PM_{10} concentration, but $PM_{2.5}$ decreased sharply.

We know that atmospheric circulation and atmospheric boundary layer structure from various numerical modeling on dust transportation and accumulation can greatly affect the dispersion and accumulation of particulate matters in the inland and coastal cities, resulting in very high pollutant concentrations [34–39]. In recent years, multivariate statistical modeling was also carried out to predict temporal and spatial analyses of particulate matter affected by gases or meteorological parameters [8,40].

Most studies for predicting the particulate matter concentrations for non-dust and dust periods have used simple regression statistical methods in Korea, except for numerical modeling [33]. We propose multiple regression statistical models to improve the predictions of PM_{10}, $PM_{2.5}$ and PM_1 concentrations for Gangneung city, Korea affected by local meteorological variables (air temperature, wind speed and relative humidity) and PM_{10} and $PM_{2.5}$ concentrations in Beijing city, China before, during and after the dust periods.

2. Study Area and Data Analysis

2.1. Study Area

Except for the summer, with its heavy precipitation, during spring, autumn, and winter, it is known that a large amount of yellow sand dusts, raised from the Gobi Desert, arid Inner Mongolia and dry regions in northern China by a strong northwesterly wind or northerly wind, are transported to the downwind regions, such as Korea, and greatly affect the local air quality of Gangneung city, showing very high concentrations of particulate matters during such dust periods [33,35,37].

As a clean city, Gangneung consists of a basin with an elevation of about 25 m above mean sea level, with high mountains over 900 m height in its west and the East Sea of Korea in its east (Figure 1). It has complicated characteristics of marine and continental climates. As this city has no special factories to emit a large amounts of air pollutants, the main atmospheric pollution sources are vehicles on the road and heating boilers in the resident area during both winter and the early spring; thus, it always maintains very low concentrations of PM, more or less 40 $\mu g/m^3$, except for during the dust period.

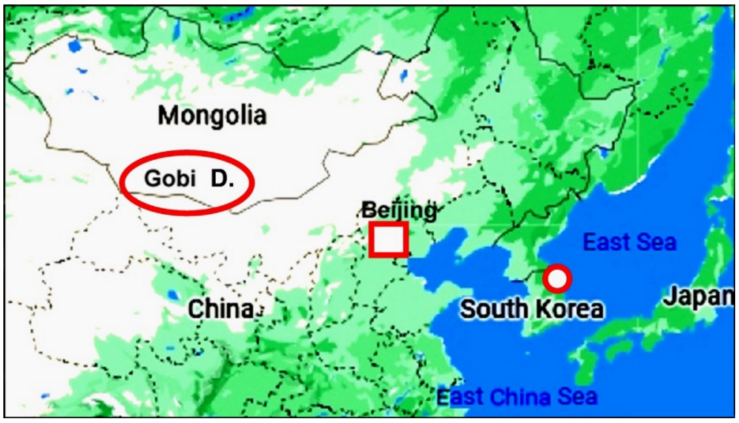

Figure 1. Topographical feature in the north-eastern Asia including the Gobi Desert (large red ellipse), Beijing city (China; red square) and Gangneung city (Korea; small red circle).

2.2. Data and Analysis

Particulate matter concentrations of PM_{10}, $PM_{2.5}$ and PM_1 were measured by a German GRIMM-1107 Dust Meter (approved by the Ministry of Environment, Korean Government), which was installed at the Gangwon Meteorological Administration (128.9° longitude; 37.75° latitude; 20 m above sea level) located in the downtown area of Gangneung city. The dust meter, devised to measure 15 sizes of dust particles (>0.3 μm to 20.0 μm), can measure the concentration of particulate matter (μg/m^3) at a 5-min interval, and the concentrations are again summed into PM_{10} (the total amount of a particle size of 10 μm or less), $PM_{2.5}$ (with the total amount of 2.5 μm size or less), and PM_1 (with the total amounts of 1 μm size or less). Then the concentrations of PM_{10}, $PM_{2.5}$, and PM_1 are recalculated as the 1 h-averaged value and these concentrations were used as the basic data for this study.

Hourly based PM_{10} and $PM_{2.5}$ data measured at Beijing city, China (especially, the South-3rd ring road observation point) were acquired through the internet with a web-site address (https://quotsoft.net/air/ or http://www.bjmemc.com.cn/ accessed on 20 March 2021). Since most of the yellow dusts, originated from the Gobi Desert and arid Inner Mongolia, pass through Beijing city to the downwind region by the northerly wind or northwesterly wind and reach Gangneung city in the eastern coast of Korea, the PM concentrations at Gangneung city are directly affected by the PM concentrations of Beijing city, still containing much of the dusts originated from the desert and arid area of northern China.

Normally, the transport time of the dusts of Beijing city to Gangneung city takes approximately two days under a relatively strong northwesterly wind of about 8 m/s to 10 m/s (i.e., over 10 m/s in the origin of the yellow dust storm), because the distance between Beijing city and Gangneung city is about 1400 km. Thus, in order to investigate the effect of PMs of Beijing city on the air quality at Gangneung city, two days early pollution data of Beijing are needed. Hourly based meteorological data measured at Gangneung, Korea were obtained from a website address (https://data.kma.go.kr/ 15 February 2021).

In this study, the correlation coefficients and predictive regression equations among PM_{10}, $PM_{2.5}$ and PM_1 of Gangneung city associated with PM_{10} and $PM_{2.5}$ of Beijing city were investigated in three divided periods of 18 March to 28 March, before the inflow of yellow dust (00:00 LST, 18 March to 00:00 LST, 21 March 2015), during the inflow (01:00 LST, 21 March to 00:00 LST, 23 March), and after the inflow (01:00 LST, 23 March to 00:00 LST, 27 March). Thus, statistical models were obtained through multiple regression analyses using IBM SPSS Statistics-25. For testing the goodness of the predicted values of PM_{10}, $PM_{2.5}$ and PM_{10} concentrations, the predicted values were compared to the observed ones.

3. Results and Discussion

3.1. Satellite Images of Yellow Dust Transport

COMS-AI (the Communication, Ocean and Meteorological Satellite, Korean Meteorological Administration (KMA)) satellite images were used to more accurately understand the real-time transport of yellow sand particles toward downwind regions. These images are very useful to verify the effect of dust particles raised from Gobi Desert passing through Beijing city, China on the local air quality of Gangneung city, Korea.

Figure 2 shows the Korean COMS-AI satellite images reflecting dust which were originated from the Gobi Desert and spread in the Gobi Desert, within its vicinity, to Inner mongo of northern China and Beijing city, and to the northern Korean peninsula at 15:00 LST (Korean Local Standard Time = UTC + 9 h) 10 March 2015 (before dust period at Gangneung city). However, the yellow dusts did not reach Gangneung city. On the other hand, after the yellow dusts reached Gangneung city, the effect of yellow dust appeared in the city, showing rapid increases in PM_{10}, $PM_{2.5}$ and PM_1 concentrations, especially in the case of PM_{10} at over 120 $\mu g/m^3$ at 21:00 LST, 21 March, and 134.67 $\mu g/m^3$ at 05:00 22 March.

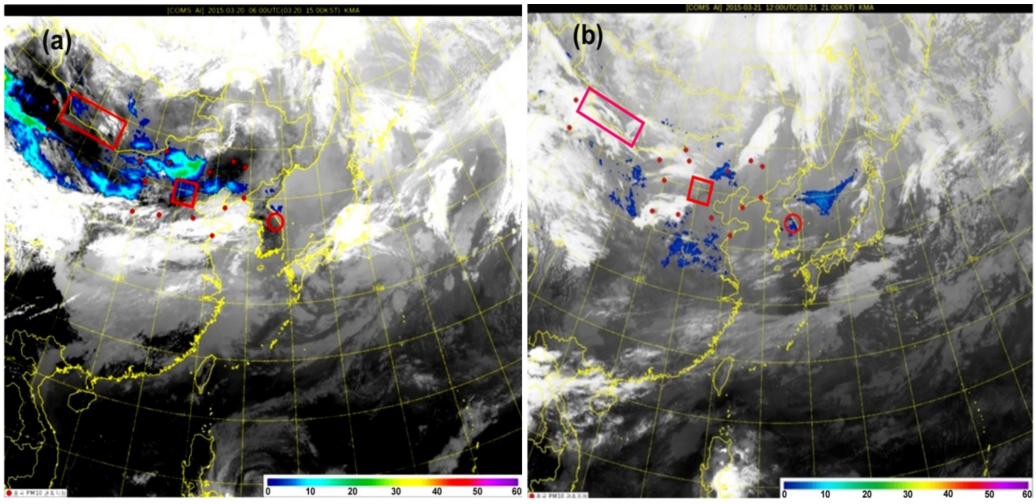

Figure 2. Korean COMS satellite images reflecting dusts at (**a**) 15:00 LST 20 March 2015 (before dust period at Gangneung city) and (**b**) 21:00 LST, 21 March (for dust period). Red small circle, small and big squares denote Gangneung (Korea), Beijing (China) and the Gobi Desert (Mongolia). (The Korea Meteorological Administration (KMA) supplied the images.) (http://www.kma.go.kr, accessed on 15 February 2021).

COMS satellite images in Figure 2 show the real-time transport of dusts raised from Gobi Desert, passing by Beijing city, China (B in Table 1) and finally reaching Gangneung city, Korea (G in Table 1) at 09:00 LST, 21 March (the starting day of the dust period). Thus, the air quality at Gangneung city can be greatly influenced by the transport of large dust particles of the Gobi Desert combined with air pollutants of Beijing city. This kind of transport pattern of the dusts continued near the end of the dust period until 00:00 LST, 23 March. Thus, except for the dust period, the air quality of this city with no factories depends upon its own pollutants from vehicles on the road and residential heating boilers.

3.2. Hourly PM_{10}, $PM_{2.5}$ and PM_1 Concentrations before, during and after the Dust Periods

In Figure 3, before the inflow of dusts from the Gobi Desert to Gangneung city (00:00 LST, March 18 to 00:00LST, March 21), the minimum concentration of PM_{10} ($PM_{2.5}$; PM_1) was 28.83 $\mu g/m^3$ (22.02 $\mu g/m^3$; 15.92 $\mu g/m^3$) and its maximum was 82.17 $\mu g/m^3$ (71.13 $\mu g/m^3$; 57.95 $\mu g/m^3$) for each hour. In contrast, during the dust period, the minimum concentration of PM_{10} ($PM_{2.5}$; PM_1) was 34.90 $\mu g/m^3$ (17.27 $\mu g/m^3$; 9.75 $\mu g/m^3$) and its maximum was 134.67 $\mu g/m^3$ (81.03 $\mu g/m^3$; 64.42 $\mu g/m^3$), respectively. After the dust

period, the minimum concentration of PM_{10} ($PM_{2.5}$; PM_1) was 19.90 μg/m^3 (1.93 μg/m^3; 7.12 μg/m^3) and its maximum was 61.58 μg/m^3 (48.25 μg/m^3; 41.53 μg/m^3), slightly less than that before the dust period.

Since most of the yellow dusts raised from the Gobi Desert and arid Inner Mongolia pass through Beijing city, China, by a northerly wind or northwesterly wind and reach Gangneung city in the eastern coast of Korea, the PM concentrations in Gangneung are directly affected by the PM concentrations of Beijing, containing much of the dusts originated from the Gobi Desert and arid area of northern China. Normally, the transport of the dusts from Beijing city to Gangneung city takes approximately two days by a prevailing northwesterly wind of about 8 m/s to 10 m/s simulated by Weather Research and Forecasting Model (WRF-3.6.1), because the distance between Beijing city and Gangneung city is about 1400 km. Thus, as the two-day earlier PM data of Beijing city correspond to the PM data of Gangneung city (Figure 4), the PM data of Gangneung city from 01:00 LST, 21 March to 00:00 LST, 23 March (during the dust period) can be affected by the PM data of Beijing city from 00:00 LST, 19 March to 01:00 LST, 21 March.

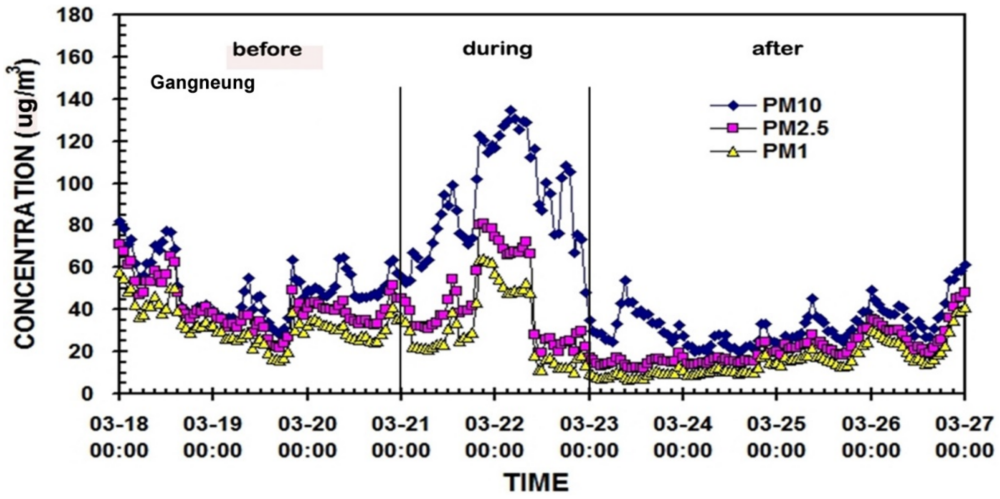

Figure 3. Hourly distribution of PM_{10}, $PM_{2.5}$ and PM_1 concentrations, before, during and after the dust period from 18 to 27 March, 2015 at Gangneung city, Korea.

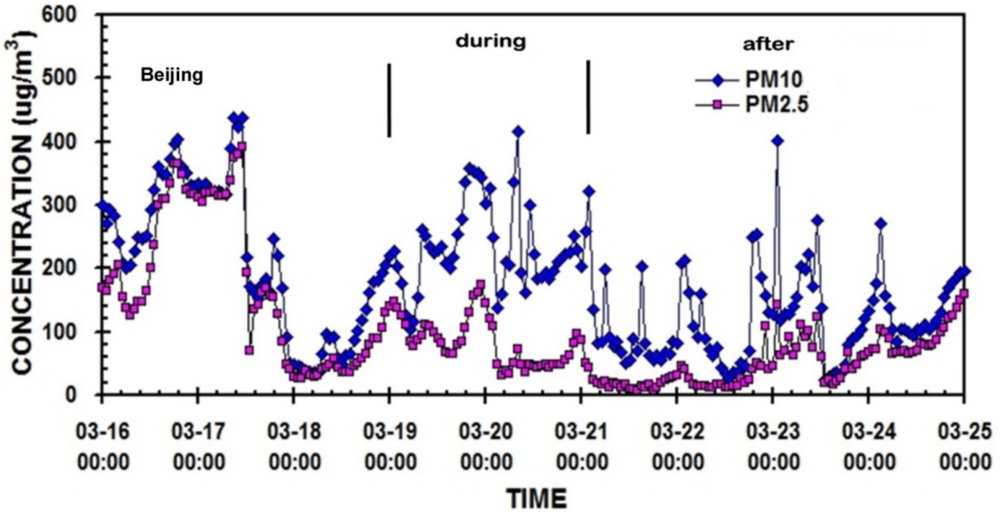

Figure 4. Hourly distribution of PM_{10}, $PM_{2.5}$ and PM_1 concentrations from 16 March to 25 March, 2015 in Beijing city, China. As the transport of the dust of Beijing city to Gangneung city takes two days by 8 m/s northwesterly wind simulated by WRF-3.6.1 numerical model, and Choi and Zhang [22], two-day-earlier PM data (01:00 LST, 19 March to 00:00 LST, 21) correspond to PM data of Gangneung city for the dust period (01:00 LST, 21 March to 00:00 LST, 23) in Figure 3.

In Gangneung city, vehicles on roads, boilers for heating and cooking in residential areas are the main sources of pollutant emissions, due to there being no factories emitting a large amount of air pollutants. The PM_{10} concentration before the yellow dust period appeared as 28.8333 to 82.1667 $\mu g/m^3$, which was 10 $\mu g/m^3$ lower or 20 $\mu g/m^3$ higher than ones of the previous case studies. When PM_{10} increased, the concentrations of $PM_{2.5}$ and PM_1 increased at the same time, and vice versa.

A very high PM concentration appeared once each in the morning and afternoon, and the concentration was particularly high at 08:00 LST to 09:00 LST (the time to go to work). The maximum concentration was shown at 20:00 LST (the time to leave the office). The high PM concentrations from 08:00 to 09:00 LST were attributed to the emission of a large amount of air pollutants, such as particulate matters and gaseous substances through the combustion of vehicle fuel and a large amount of dust scattered by the movement of the vehicles on the road.

Similarly, at 20:00 LST or 22:00 LST (two or three hours after the time to leave work), the PM concentration was also very high, with a maximum concentration. It was due to a large amount of both particulate matters and gaseous emitted from vehicles and scattered dust flied from the road, and added air pollutants emitted from boilers for heating and cooking in the resident area under the relative cool weather in the early evening in the city in March.

During the daytime after 09:00 LST, PM concentration was generally low. Choi and Speer [16] reported that as the ground surface is heated by the solar radiation, the heated air rises vertically, accompanying the air pollutants emitted from vehicles and fling dusts on the road to the top of the atmospheric boundary layer d to about 1 km height, resulting in the low concentrations of particulate and gaseous. Differently, as the nocturnal surface inversion layer (NSIL) is formed with a very compressed thin layer of about 200 m in height, due to the ground surface cooling (called a strong stable layer). This temperature structure can induce the falling of air toward the ground surface and accumulation of pollutants near the surface, an increase in the pollutant concentration, occurs with a maximum concentration of PM at 22:00 LST, similar to previous cases with a deviated occurrence time [35,37]. After that, the PM concentration is lowered, because the amount of air pollutants emitted from the vehicles is decreased, due to the decreased number of vehicles at night after 22:00 LST.

Figure 5 shows the hourly distributions of the air temperature (°C), wind speed (m/s) and relative humidity (%), corresponding to PMs concentrations from 18 to 27 March, 2015 in Gangneung, Korea. It is well known that when yellow dusts are raised up from the dry ground surface of the Gobi Desert, the relative humidity in air near the ground surface is less than 40% and the wind speed is over 10 m/s. A northwesterly wind of more or less 10 m/s transports the yellow dusts toward the downwind regions, such as Gangneung city, Korea.

During the dust period in Gangneung city on 21 to 22 March, 2015, the air temperature was high, and visibility was low, but the wind speed was relatively high at about 4 m/s to 6m/s. Namely, as air temperature and wind speed increase, PM_{10}, $PM_{2.5}$ and PM_1 concentrations also increase, concurrently, while relative humidity decreases (Figures 3 and 5). Even though the northwesterly wind over 10 m/s in the source origin of yellow dusts was reduced to 4 m/s to 6 m/s in Gangneung city, still the strong wind could transport the yellow dusts into this city and simultaneously easily raise up dust particles on the road to the low atmosphere of the city.

For instance, on 19 March, as the relative humidity at Gangneung city was over 90%, PM_{10}, $PM_{2.5}$ and PM_1 concentrations were very low, showing their minima. On the other hand, when the relative humidity was less than 30% on 21 and 22 March, very high concentrations of PM_{10}, $PM_{2.5}$ and PM_1 were detected with their maxima. Thus, it means that those meteorological variables have strong correlations with the particulate matter concentrations.

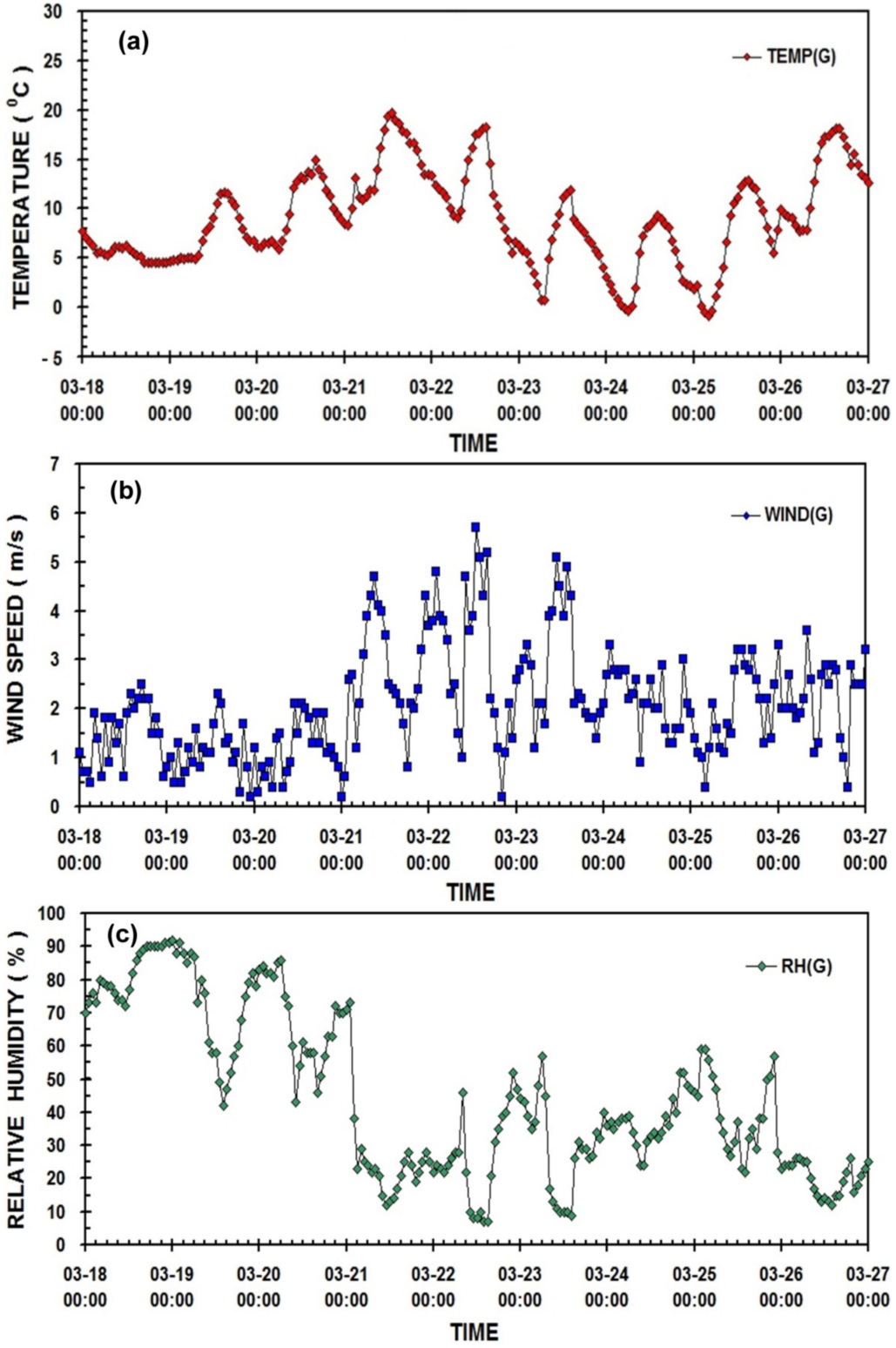

Figure 5. Hourly distributions of (**a**) air temperature (°C), (**b**) wind speed (m/s) and (**c**) relative humidity (%) corresponding to PMs concentrations from 18 March to 27, 2015 in Gangneung city, Korea.

3.3. Correlation Matrix and Predictive Regression Equations among PM_{10}, $PM_{2.5}$ and PM_1 (Gangneung) Associated with PM_{10} and $PM_{2.5}$ (Beijing)

In linear regression, there is only one independent and dependent variable involved, but, in the case of multiple regression, there is a set of independent variables X_j to explain

better or predict the dependent variable, Y_i. The applied models for the prediction of values have the forms of a multiple predictive regression equation of each PM_{10}(G), $PM_{2.5}$(G) and PM_1(G) concentration of Gangneung city influenced by the local meteorological parameters and the PM_{10}(B) and $PM_{2.5}$(B) concentrations of Beijing city, shown in Table 2.

$$Y_1 = a_{11}X_1 + a_{12}X_2 + a_{13}X_3 + a_{14}X_4 + a_{15}X_5 + a_{16}X_6 + a_{17}X_7 + a_{18}X_8 + b_1$$

$$Y_2 = a_{21}X_1 + a_{22}X_2 + a_{23}X_3 + a_{24}X_4 + a_{25}X_5 + a_{26}X_6 + a_{27}X_7 + a_{28}X_8 + b_2$$

$$Y_3 = a_{31}X_1 + a_{23}X_2 + a_{33}X_3 + a_{43}X_4 + a_{53}X_5 + a_{63}X_6 + a_{73}X_7 + a_{83}X_8 + b_3 \quad (1)$$

or

$$Y_i = a_{ij}X_{ij} + b_i \quad (2)$$

where a_{ij} (i = 1 to 3, j = 1 to 8) means the coefficient of matrix (here, a_{11}, a_{22} and a_{33} are zero). The observed values of X_j (j = 1 to 8) are PM_{10}(G), $PM_{2.5}$(G), PM_1(G), T(G, air temperature), W(G, wind speed), RH(G, relative humidity), PM_{10}(B) and $PM_{2.5}$(B) as independent variables. The predictive values of Y_i (i = 1 to 3) are PM_{10}(G), $PM_{2.5}$(G) and PM_{10}(G)) as dependent variables. b_i (i = 1 to 3) are intercepts in the equations of Y_i as the error term, respectively. The final multiple regression equations are given in Table 1.

Table 1 indicates that multiple correlation coefficients are present among PMs, and meteorological parameters (air temperature, T; wind speed, W; and relative humidity, RH) of Gangneung city (Korea) are associated with the PMs of Beijing city. Additionally, predictive regression equations of each PM concentration at Gangneung city before, during after the dust periods and all periods are shown. Multivariate statistical modeling for evaluating the predicted values of the PMs of Gangneung was performed in four classifications of period via multiple regression analyses, using IBM SPSS Statistics-25.

Multiple correlation coefficients among PM_{10}(G) $PM_{2.5}$(G) and PM_1(G) were in the range of 0.916 to 0.998. In particular, the correlation coefficients of PM_{10}(G), $PM_{2.5}$(G) and PM_1(G) before, during and after the dust periods were 0.983 to 0.998, 0.916 to 0.998 and 0.941 to 0.998, respectively. However, for all periods, those coefficients were 0.954 to 0.998, showing perfect correlations. Except for the slightly lower coefficients (0.916, 0.941) of PM_{10} during and after the dust periods, the correlation coefficient of any PM concentration was in the range of 0.954 to 0.998.

Correlation analysis showed that PM_{10}(G) $PM_{2.5}$(G), PM_1(G), T(G), W(G), RH(G), PM_{10}(B), $PM_{2.5}$(B) were significantly correlated at $p < 0.001$, though the correlation coefficients were different. Regardless of non-dust and dust periods, in particular, the correlation coefficients of both $PM_{2.5}$ and PM_1 were in the range of 0.997 to 0.998, showing perfect correlations.

3.4. Partial Correlation Matrix among PMs of Gangneung (G) and PMs of Beijing (B)

Table 2 presents the partial correlation coefficients (Pearson r) of PMs associated with the meteorological parameters of Gangneung (Korea) and PMs of Beijing (China), before, during, and after the dust periods and all periods. The partial correlation coefficients among PM_{10}, $PM_{2.5}$ and PM_1 concentrations in Table 2 are much lower than the multiple correlation coefficients among them in Table 1, before, during and after the dust periods, except for the correlation coefficients of PM_{10}(G) and $PM_{2.5}$(G).

This implies that the calculated values of each PM concentration using multiple regression statistical models are much closer to the observed values for non-dust and dust periods, in Table 1. The highest coefficient (the lowest) between PM_{10} and $PM_{2.5}$ at Gangneung city was 0.913 before the dust period (0.725 during the dust period), and the highest coefficient (the lowest) between $PM_{2.5}$ and PM_1 was 0.997 after the dust period (0.989 before the dust period).

Table 1. Multiple correlation coefficients and predictive regression equations among PMs of Gangneung city (G) with PMs of Beijing city (B) under the influence of meteorological parameters. T, W and RH denote air temperature (°C), wind speed (m/s) and relative humidity (%).

Period	Multi-Correlation Coefficient	Predictive Regression Equation
18/03/2015 to 21/03/2015 (Before dust period)	0.983	$PM_{10}(G) = 3.353 \times PM_{2.5}(G) - 2.708 \times PM_1(G) + 0.601 \times T(G) - 1.240 \times W(G) + 0.009 \times RH(G) - 0.006 \times PM_{10}(B) + 0.002 \times PM_{2.5}(B) - 2.206$
	0.998	$PM_{2.5}(G) = 0.211 \times PM_{10}(G) + 0.917 \times PM_1(G) - 0.245 \times T(G) + 0.269 \times W(G) - 0.035 \times RH(G) + 0.006 \times PM_{10}(B) - 0.007 \times PM_{2.5}(B) + 4.638$
	0.997	$PM_1(G) = -0.193 \times PM_{10}(G) + 1.038 \times PM_{2.5}(G) + 0.258 \times T(G) - 0.240 \times W(G) + 0.049 \times RH(G) - 0.005 \times PM_{10}(B) + 0.006 \times PM_{2.5}(B) - 5.710$
21/03/2015 to 23/03/2015 (During dust period)	0.916	$PM_{10}(G) = 3.560 \times PM_{2.5}(G) - 3.114 \times PM_1(G) - 0.914 \times T(G) + 4.444 \times W(G) - 0.360 \times RH(G) + 0.082 \times PM_{10}(B) - 0.252 \times PM_{2.5}(B) + 42.893$
	0.998	$PM_{2.5}(G) = 0.047 \times PM_{10}(G) + 1.166 \times PM_1(G) - 0.043 \times T(G) - 0.525 \times W(G) - 0.009 \times RH(G) - 0.001 \times PM_{10}(B) - 0.019 \times PM_{2.5}(B) + 7.359$
	0.998	$PM_1(G) = -0.030 \times PM_{10}(G) + 0.842 \times PM_{2.5}(G) + 0.042 \times T(G) + 0.406 \times W(G) + 0.009 \times RH(G) + 0.001 \times PM_{10}(B) + 0.020 \times PM_{2.5}(B) - 6.874$
23/03/2015 to 27/03/2015 (After dust period)	0.941	$PM_{10}(G) = 6.841 \times PM_{2.5}(G) - 6.102 \times PM_1(G) - 0.548 \times T(G) + 1.859 \times W(G) - 0.433 \times RH(G) - 0.008 \times PM_{10}(B) + 0.002 \times PM_{2.5}(B) - 1.628$
	0.998	$PM_{2.5}(G) = 0.090 \times PM_{10}(G) + 0.946 \times PM_1(G) + 0.061 \times T(G) - 0.182 \times W(G) + 0.044 \times RH(G) + 0.002 \times PM_{10}(B) - 0.001 \times PM_{2.5}(B) + 1.747$
	0.998	$PM_1(G) = -0.088 \times PM_{10}(G) + 1.042 \times PM_{2.5}(G) - 0.060 \times T(G) + 0.185 \times W(G) - 0.043 \times RH(G) - 0.002 \times PM_{10}(B) + 0.003 \times PM_{2.5}(B) - 1.908$
18/03/2015 to 27/03/2015 (all periods)	0.954	$PM_{10}(G) = 5.826 \times PM_{2.5}(G) - 5.670 \times PM_1(G) + 0.554 \times T(G) + 3.456 \times W(G) - 0.112 \times RH(G) + 0.039 \times PM_{10}(B) - 0.018 \times PM_{2.5}(B) - 12.128$
	0.998	$PM_{2.5}(G) = 0.104 \times PM_{10}(G) + 1.059 \times PM_1(G) - 0.003 \times T(G) - 0.328 \times W(G) + 0.019 \times RH(G) + 0.005 \times PM_{10}(B) - 0.010 \times PM_{2.5}(B) + 1.350$
	0.997	$PM_1(G) = -0.088 \times PM_{10}(G) + 0.924 \times PM_{2.5}(G) + 0.006 \times T(G) + 0.268 \times W(G) - 0.014 \times RH(G) - 0.005 \times PM_{10}(B) + 0.010 \times PM_{2.5}(B) - 1.246$

Before the dust period, PM_{10} of Gangneung city is positively influenced by its relative humidity, but it is negatively by the local air temperature, wind speed, PM_{10} and $PM_{2.5}$ of Beijing. $PM_{2.5}$ of Gangneung city is positively influenced by its relative humidity and the PM_{10} of Beijing city, but it is negatively by others. PM_1 is negatively influenced by the local air temperature and wind speed, except for others.

During the dust period, PM_{10} of Gangneung is positively influenced by the local air temperature, wind speed and PM_{10} of Beijing, except for others. The $PM_{2.5}$ concentration is negatively influenced by the local wind speed and relative humidity, except for others. PM_1 of Gangneung city is positively influenced by all variables. After the dust period, PM_{10} of Gangneung city is negatively influenced by the local relative humidity, except for others. $PM_{2.5}$ and PM_1 at Gangneung city are negatively influenced by the local wind speed and relative humidity, except for others. For all periods, PM_{10} of Gangneung city is negatively influenced by the local relative humidity, except for others, but $PM_{2.5}$ and PM_1 are negatively influenced by the local wind speed, except for others.

In particular, the air quality of Gangneung city during the dust period becomes seriously worse due to the huge amounts of transported dusts (mainly composed of coarse particles larger than 2.5 μm in diameter) from the Gobi Desert passing through Beijing city, as shown in Figure 2. Correlation coefficients of PM_{10} between $PM_{2.5}$ and PM_1 at Gangneung city are high with 0.913 and 0.854 (before the dust period), 0.725 and 0.689 (during the dust period), 0.732 and 0.709 (after the dust period), and 0.767 and 0.685 (all periods).

Table 2. Partial correlation matrix among PMs associated with meteorological parameters of Gangneung city (G) and PMs of Beijing city (B), before, during and after the dust periods.

Period	Item	PM_{10} (G)	$PM_{2.5}$ (G)	PM_1 (G)	Temp (G)	Wind (G)	RH (G)	PM_{10} (B)	$PM_{2.5}$ (B)
Before	PM_{10} (G)	1.000	0.913	0.854	−0.112	−0.218	0.019	−0.035	−0.260
	$PM_{2.5}$ (G)		1.000	0.989	−0.385	−0.150	0.320	0.210	−0.003
	PM_1 (G)			1.000	−0.444	−0.132	0.403	0.267	0.067
	Temp (G)				1.000	0.100	−0.897	−0.701	−0.694
	Wind (G)					1.000	−0.009	0.084	0.131
	RH (G)						1.000	0.623	0.644
	PM_{10} (B)							1.000	0.952
	$PM_{2.5}$ (B)								1.000
During	PM_{10} (G)	1.000	0.725	0.689	0.117	0.244	−0.286	0.407	−0.119
	$PM_{2.5}$ (G)		1.000	0.996	0.030	−0.013	−0.007	0.567	0.411
	PM_1 (G)			1.000	0.041	0.005	−0.005	0.574	0.466
	Temp (G)				1.000	0.395	−0.794	0.060	−0.021
	Wind (G)					1.000	−0.651	−0.103	−0.056
	RH (G)						1.000	0.112	0.226
	PM_{10} (B)							1.000	0.459
	$PM_{2.5}$ (B)								1.000
After	PM_{10} (G)	1.000	0.732	0.709	0.419	0.212	−0.470	0.279	0.584
	$PM_{2.5}$ (G)		1.000	0.997	0.346	−0.180	−0.111	0.391	0.847
	PM_1 (G)			1.000	0.356	−0.171	−0.127	0.372	0.846
	Temp (G)				1.000	0.209	−0.741	−0.167	0.344
	Wind (G)					1.000	−0.475	−0.095	−0.225
	RH (G)						1.000	0.190	−0.110
	PM_{10} (B)							1.000	0.551
	$PM_{2.5}$ (B)								1.000
All	PM_{10} (G)	1.000	0.767	0.685	0.453	0.247	−0.166	0.458	0.091
	$PM_{2.5}$ (G)		1.000	0.990	0.217	−0.121	0.273	0.583	0.425
	PM_1 (G)			1.000	0.179	−0.158	0.325	0.580	0.479
	Temp (G)				1.000	0.355	−0.548	−0.036	−0.133
	Wind (G)					1.000	−0.623	−0.100	−0.281
	RH (G)						1.000	0.391	0.629
	PM_{10} (B)							1.000	0.780
	$PM_{2.5}$ (B)								1.000

PM_{10}, $PM_{2.5}$ and PM_1 at Gangneung during the dust period are highly correlated with PM_{10} at Beijing with 0.407, 0.567 and 0.574, in contrast to other periods. It means that when PM_{10} of Beijing increased, those concentrations of Gangneung also increased. As a result, the effect of PM_{10} of Beijing city exists, when the PMs of Gangneung increases. However, both $PM_{2.5}$ and PM_1 concentrations of Gangneung were still positively influenced by $PM_{2.5}$ of Beijing, except for PM_{10}, having a negative sign. From the above statement, the long-distance transport of dust particles from Beijing, China to Gangneung, Korea is very significant to the variation in the air quality of Gangneung.

3.5. Validation of Models

Figure 6 indicates the comparison between the observed values and the predicted values calculated by multiple predictive regression models in Table 1. In order to test the goodness of the estimations of each PM concentration, the scattered diagrams show model fitting with calculated and observed PM_{10}, $PM_{2.5}$ and PM_1 concentrations. Their original observed values were reproduced by the comparison of observed values with calculated values, before, during, after the dust periods and for all periods. The reproduced observed values can be calculated by the linear regression equations in the scattered diagrams of Figure 6.

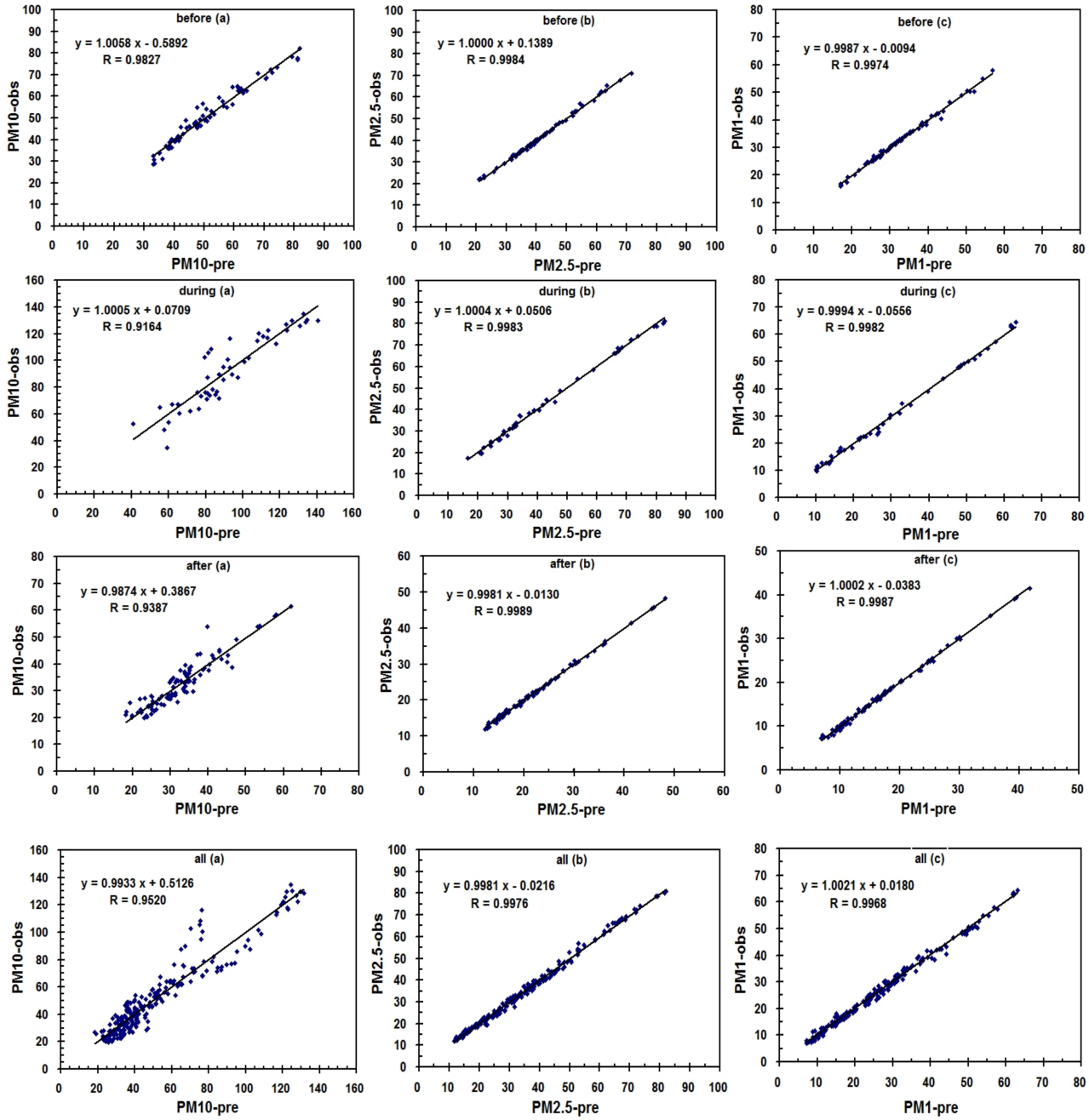

Figure 6. Comparison of observed with calculated PM_{10}, $PM_{2.5}$ and PM_1 values in (**a**–**c**) figures before, during and after the dust periods and all periods from 18 March to 21, 2015 at Gangneung city, Korea.

Figure 7 shows that each observed and calculated PM value with the date denotes the behavior throughout each period. The correlation coefficient of each PM concentration in

the scattered diagram is slightly improved over the correlation coefficient in Table 1, in the case of the PM_{10} concentration after the dust period and all periods.

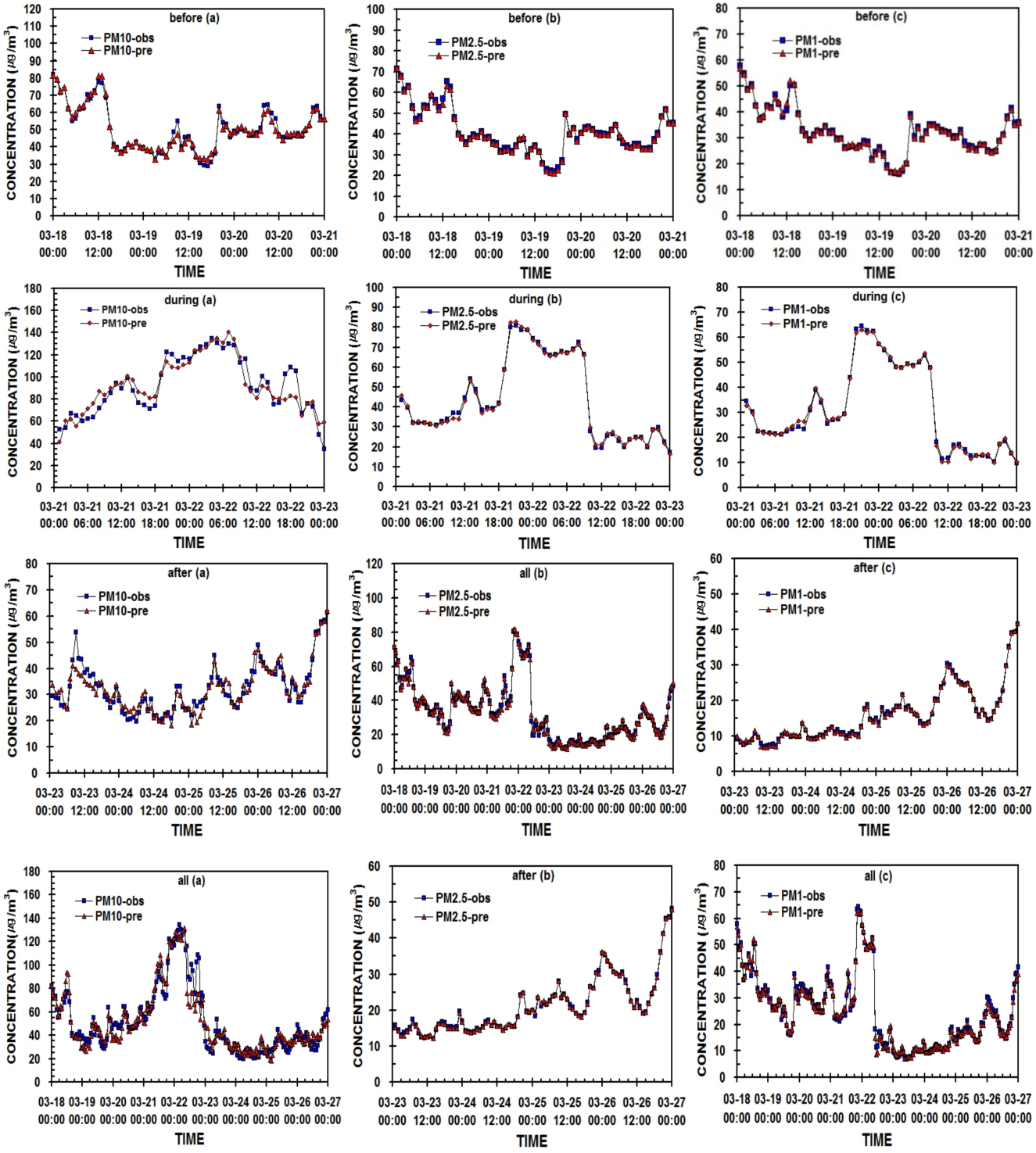

Figure 7. The comparison of observed vs. calculated PM_{10}, $PM_{2.5}$ and PM_1 values with date in (**a**–**c**) figures through model fitting, before, during, after the dust periods and all periods from 18 to 27 March, 2015 in Gangneung city, Korea.

4. Conclusions

The multivariate statistical modeling among hourly PM_{10}, $PM_{2.5}$ and PM_1 concentrations in Gangneung city, Korea, influenced by the local meteorological parameters and

PM_{10} and $PM_{2.5}$ concentrations in Beijing city, China, was performed for non-dust and dust periods in March, and it gave the following results.

1. Before and after the dust period, PM_{10}, $PM_{2.5}$ and PM_1 concentrations showed as being very high at 09:00 LST of the morning rush hour by the increasing of the emitted pollutants from vehicles on the road. Their maxima values were detected at 20:00 to 22:00 LST of the evening departure time, with additional pollutants from resident heating boilers. However, during the dust period, these peak trends were not found under the persistent accumulation of dusts and particulate matters in Gangneung city from the Gobi Desert and Beijing city.
2. Correlation coefficients among PM_{10}, $PM_{2.5}$ and PM_1 in Gangneung, using multiple regression statistical models, were in the range of 0.916 to 0.998, and the significant level of the regression was $p < 0.001$, showing all the coefficients to be significant.
3. Before the dust period, PM_{10} of Gangneung city is positively influenced by its relative humidity, but it is negatively by the local air temperature, wind speed, PM_{10} and $PM_{2.5}$ of Beijing. $PM_{2.5}$ of Gangneung city is positively influenced by its relative humidity and PM_{10} of Beijing, but it is negatively influenced by others. PM_1 is negatively influenced by its air temperature and wind speed, except for others.
4. During the dust period, PM_{10} of Gangneung city is positively influenced by the local air temperature, wind speed and PM_{10} of Beijing, except for others. $PM_{2.5}$ concentration is negatively influenced by the local wind speed and relative humidity, except for others. PM_1 of Gangneung is positively influenced by all variables.
5. After the dust period, PM_{10} of Gangneung city is negatively influence by local relative humidity, except for others. $PM_{2.5}$ and PM_1 in Gangneung city are negatively influenced by the local wind speed and relative humidity, except for others. For all periods, PM_{10} of Gangneung city is negatively influence by the local relative humidity, except for others, but $PM_{2.5}$ and PM_1 are negatively influenced by the local wind speed, except for others.
6. Multivariate statistical models were devised to predict each PM concentration. The observed and calculated PM concentrations were compared each other, and new linear regression prediction models to reproduce the original observed PM values were also suggested.

Author Contributions: Conceptualization, S.-M.C. and H.C.; methodology, S.-M.C. and H.C.; software, S.-M.C. and H.C.; validation, S.-M.C. and H.C.; formal analysis S.-M.C. and H.C.; investigation, S.-M.C. and H.C.; resources, S.-M.C. and H.C.; data curation, S.-M.C. and H.C.; writing—original draft preparation, S.-M.C. and H.C.; writing—review and editing, H.C.; supervision, H.C.; project administration, H.C. All authors have read and agreed to the published version of the manuscript.

Funding: This research received no external funding.

Data Availability Statement: Hourly based PM_{10} and $PM_{2.5}$ data measured at Beijing (especially, the South-3rd ring road observation point), China were acquired through internet with a website address (https://quotsoft.net/air/ or http://www.bjmemc.com.cn/ accessed on 20 March 2021). Hourly based meteorological data measured at Gangneung, Korea and satellite images were obtained from website addresses of the KMA (https://data.kma.go.kr/; http://www.kma.go.kr accessed on 15 February 2021).

Acknowledgments: The authors express much thanks to the Beijing Municipal Ecological and Environmental Monitoring Center for obtaining air quality data in the Beijing district and to the Korea Meteorological Administration for the meteorological data and satellite images in support of this work.

Conflicts of Interest: The authors declare no conflict of interest.

References

1. Westerholm, R.; Almen, J.; Li, H.; Rannug, U.; Rosen, A. Exhaust emission from gasoline-fulled light duty vehicle operated in different driving conditions; a chemical and biological characterization. *Atmos. Environ. B* **1992**, *26*, 79–90. [CrossRef]

2. Li, C.; Dai, Z.; Yang, L.; Ma, Z. Spatiotemporal characteristics of air quality across Weifang from 2014–2018. *Int. J. Environ. Res. Public Health* **2019**, *16*, 3122. [CrossRef]
3. Chow, J.C. Health effects of fine particulate air pollution; Lines that connect. *J. Air Waste Manag. Assoc.* **2006**, *56*, 707–708. [CrossRef] [PubMed]
4. Huang, D.; Xu, J.; Zhang, S. Valuing the health risks of particulate air pollution in the Pearl River Delta, China. *Environ. Sci. Policy* **2012**, *15*, 38–47. [CrossRef]
5. Shen, F.; Ge, X.; Hu, J.; Nie, D.; Tian, L.; Chen, M. Air pollution characteristics and health risks in Henan Province, China. *Environ. Res. Sci.* **2017**, *156*, 625–634. [CrossRef] [PubMed]
6. Bhaskar, B.V.; Mehta, V.M. Atmospheric particulate pollutants and their relationship with meteorology in Ahmedabad. *Aerosol Air Qual. Res.* **2010**, *10*, 301–315. [CrossRef]
7. Cheng, Y.; He, K.B.; Du, Z.Y.; Zheng, M.; Duan, F.K.; Ma, Y.L. Humidity plays an important role in the $PM_{2.5}$ pollution in Beijing. *Environ. Pollut.* **2015**, *197*, 68–75. [CrossRef]
8. Li, X.; Ma, Y.; Wang, Y.; Liu, N.; Hong, Y. Temporal and spatial analyses of particulate matter (PM_{10} and $PM_{2.5}$) and its relationship with meteorological parameters over an urban city in northeast China, 2017. *Atmos. Res.* **2017**, *198*, 185–193. [CrossRef]
9. Shi, C.; Yuan, R.; Wu, B.; Meng, Y.; Zhang, H.; Zhang, H.; Gong, Z. Meteorological conditions to $PM_{2.5}$ pollution in winter 2016/2017 in the western Yangtze River Delta, China. *Sci. Total Environ.* **2018**, *642*, 1221–1232. [CrossRef] [PubMed]
10. Park, D.; Ha, K. Characteristics of PM_{10}, $PM_{2.5}$, CO_2 and CO monitored in interiors and platforms of subway train in Seoul, Korea. *Environ. Int.* **2008**, *34*, 629–634. [CrossRef] [PubMed]
11. Zhao, S.; Yu, Y.; Yin, D.; He, J.; Liu, N.; Qu, J.; Xiao, J. Annual and diurnal variations of gaseous and particulate pollutants in 31 provincial capital cities based on in sit air quality monitoring data from China National Environmental Monitoring Center. *Environ. Int.* **2016**, *86*, 92–106. [CrossRef] [PubMed]
12. Ma, X.; Jia, H. Particulate matter and gaseous pollutions in three megacities over China: Situation and implication. *Atmos. Environ.* **2016**, *140*, 476–494. [CrossRef]
13. Xiao, K.; Wang, Y.K.; Wu, G.; Fu, B.; Zhu, Y. Spatiotemporal characteristics of air pollutions (PM_{10}, $PM_{2.5}$, SO_2, NO_2, O_3, and CO) in the inland basin city of Chengdu, Southwest China. *Atmosphere* **2018**, *9*, 74. [CrossRef]
14. Li, F.; Liu, Y.; Lu, J.J.; Liang, L.; Harmer, P. Ambient air pollution in China poses a multi-faceted health threat to outdoor physical activity. *J. Epidemiol. Community Health* **2015**, *69*, 201–204. [CrossRef]
15. He, J.Q.; Yu, X.N.; Zhu, B.; Yuan, L.; Ma, J.; Shen, L.; Zhu, J. Characteristics of Aerosol Extinction and Low Visibility in Haze Weather in Winter of Nanjing, China. *Environ. Sci.* **2016**, *36*, 1645–1653. Available online: http://www.zghjkx.com.cn/EN/abstract/abstract14655.shtml (accessed on 20 March 2021).
16. Choi, H.; Speer, M.S. Effects of atmospheric circulation and boundary layer structure on the dispersion of suspended particulates in the Seoul metropolitan area. *Meteorol. Atmos. Phys.* **2006**, *92*, 239–254. [CrossRef]
17. Zhang, X.; Arimoto, R.; An, Z.; Chen, T.; Zhang, G.; Zhu, G.; Wang, X. Atmospheric trace elements over source regions for Chinese dust: Concentrations, sources and atmospheric deposition on the Loess Plateau. *Atmos. Environ.-A* **1993**, *27*, 2051–2067. [CrossRef]
18. Chung, Y.; Yoon, M. On the Occurrence of Yellow Sand and Atmospheric Loadings. *Atmos. Environ.* **1996**, *30*, 2387–2397. Available online: http://www.koreascience.or.kr/article/JAKO199411921388674.page (accessed on 20 June 2021). [CrossRef]
19. Chung, Y.S.; Kim, H.S.; Natsagdorj, L.; Jugder, D.; Chen, S.J. On Yellow Sand Occurred During 1997–2000. *J. Korean Meteorol. Sci.* **2001**, *37*, 305–316. Available online: https://www.dbpia.co.kr/journal/articleDetail?nodeId=NODE00952163 (accessed on 20 June 2021).
20. Wang, X.; Ma, Y.; Chen, H.; Wen, G.; Chen, S.; Tao, Z.; Chung, Y. The relation between sandstorms and strong winds in Xinjiang, China. *Water Air Soil Pollut.* **2003**, *3*, 67–79. [CrossRef]
21. Zhang, Y.; Zhong, Y. The simulation and diagnosis for a strong wind associated northeast low. *Acta Meteorol. Sin.* **1985**, *43*, 97–105.
22. Choi, H.; Zhang, Y.H. Predicting duststorm evolution with the vorticity theory. *Atmos. Res.* **2008**, *89*, 338–350. [CrossRef]
23. Tegen, I.; Fung, I. Modeling of mineral dust in the atmosphere: Sources, transport, and optical thickness. *J. Geophys. Res.-D* **1994**, *99*, 22897–22914. [CrossRef]
24. Kotamarthi, V.R.; Carmichael, G.R. The long range transport of pollutants in the Pacific Rim region. *Atmos. Environ.-A* **1990**, *24*, 1521–1534. [CrossRef]
25. McKendry, I.G.; Hacker, J.P.; Stull, R.; Sakiyama, S.; Mignacca, D.; Reid, K. Long-range transport of Asian dust to the Lower Fraser Valley, British Columbia, Canada. *J. Geophys. Res. Atmos.-D* **2001**, *106*, 18361–18370. [CrossRef]
26. Lin, T. Long-range transport of yellow sand to Taiwan in Spring 2000: Observed evidence and simulation. *Atmos. Environ.* **2001**, *35*, 5873–5882. [CrossRef]
27. Carmichael, G.R.; Hong, M.; Ueda, H.; Chen, L.; Murano, K.; Park, J.K.; Lee, H.; Kim, Y.; Kang, C.; Shim, S. Aerosol composition at Cheju Island, Korea. *J. Geophys. Res.-D* **1997**, *102*, 6047–6061. [CrossRef]
28. Kim, Y.J.; Kim, K.W.; Kim, S.D.; Lee, B.K.; Han, J.S. Fine particulate matter characteristics and its impact on visibility impairment at two sites in Korea: Seoul and Incheon. *Atmos. Environ.* **2000**, *40*, 593–609. [CrossRef]
29. Choi, H. Characteristics of Hourly Variation of Gaseous Pollutant Concentration at Gangneung, Korea for Yellow Sand Event Period in Winter Case Study of 14–16 February 2005. *J. Clim. Res.* **2011**, *6*, 59–76. Available online: https://www.kci.go.kr/kciportal/ci/sereArticleSearch/ciSereArtiView.kci?sereArticleSearchBean.artiId=ART001533093 (accessed on 20 June 2021).

30. Zhao, D.; Chen, H.; Yu, E.; Luo, T. $PM_{2.5}/PM_{10}$ ratios in eight economic regions and their relationship with meteorology in China. *Adv. Meteorol.* **2019**, *15*, 5296725. [CrossRef]
31. Choi, H. Comparison of PM_1, $PM_{2.5}$ and PM_{10} concentrations in a mountainous coastal city, Gangneung before and after the Yellow Dust event in spring. *J. Environ. Sci.* **2008**, *17*, 633–645. [CrossRef]
32. Choi, H. Impact of Fine Particulate Matters Transported from Gobi Desert to Particulate Concentrations (PM_{10}, $PM_{2.5}$, PM_1) for Yellow Sand Event Period in Fall-Case study of 27 October 2003. *J. Clim. Res.* **2010**, *5*, 219–233. Available online: https://www.kci.go.kr/kciportal/ci/sereArticleSearch/ciSereArtiView.kci?sereArticleSearchBean.artiId=ART001493480 (accessed on 20 June 2021).
33. Lee, M.S.; Chung, J.D. Impact of yellow dust transport from Gobi Desert on fractional ratio and correlations of temporal PM_{10}, $PM_{2.5}$ and PM1 at Gangneung city in fall. *J. Environ. Sci.* **2012**, *21*, 217–231. [CrossRef]
34. Choi, H.; Zhang, Y.H.; Takahashi, S. Recycling of suspended particulates by the interaction of sea-land breeze circulation and complex coastal terrain. *Meteorol. Atmos. Phys.* **2004**, *87*, 109–120. [CrossRef]
35. Choi, H.; Choi, D.S. Concentrations of PM_{10}, $PM_{2.5}$, and PM_1 influenced by atmospheric circulation and atmospheric boundary layer in the Korean mountainous coast during a duststorm. *Atmos. Res.* **2008**, *89*, 330–337. [CrossRef]
36. Choi, H.; Zhang, Y.H.; Kim, K.H. Sudden high concentration of TSP affected by atmospheric boundary layer in Seoul metropolitan area during duststorm period. *Environ. Int.* **2008**, *34*, 635–647. [CrossRef] [PubMed]
37. Choi, H.; Choi, D.S.; Choi, S.M. Meteorological condition and atmospheric boundary layer influenced upon temporal concentrations of PM_1, $PM_{2.5}$ at a Coastal City, Korea for Yellow Sand Event from Gobi Desert. *Dis. Adv.* **2010**, *3*, 309–315.
38. Uzan, L.; Alpert, P. The coastal boundary layer and air pollution—A high temporal resolution analysis in the East Mediterranean coast. *Open Atmos. Sci. J.* **2012**, *6*, 9–18. [CrossRef]
39. Choi, H. Trapping effect of a calm zone by lee side-internal gravity waves and cyclonic winds on sudden high concentrations of particulate matters combined with the Yellow Dusts from Gobi Desert in the Korean eastern coast. *Dis. Adv.* **2013**, *6*, 101–111.
40. He, J.H.; Ding, S.; Liu, D.F. Exploring the spatiotemporal pattern of $PM_{2.5}$ distribution and its determinants in Chinese cities based on a multilevel analysis approach. *Sci. Total Environ.* **2019**, *659*, 1513–1525. [CrossRef]